Effect of Temperature on Fracture Toughness of PC/ABS Based on *J*-Integral and Hysteresis Energy Methods

MING-LUEN LU, KUO-CHAN CHIOU, and FENG-CHIH CHANG*

Institute of Applied Chemistry, National Chiao Tung University, Hsin-Chu, Taiwan, Republic of China

SYNOPSIS

The critical fracture toughness J_{1c} of the polycarbonate (PC)/acrylonitrile–butadiene–styrene (ABS) blend at different temperatures was obtained from ASTM E813-81, E813-87, and the recently developed hysteresis energy methods, respectively. The J_{1c} value increases with increase of the test temperature ranging from −60 to 70°C. The hysteresis energy method and the ASTM E813-81 method result in comparable J_{1c} values, while the ASTM E813-87 results in about 80–110% higher values. The critical initiation displacements determined from the plots of hysteresis energy and the true crack growth length vs. crosshead displacement are very close. This indicates that the critical initiation displacement determined by the hysteresis method is indeed the displacement at the onset of true crack initiation and the corresponding J_{1c} represents a physical event of crack initiation. The fracture toughness, K_{1c} value, based on linear elastic fracture mechanics (LEFM), was determined by using K_Q analysis (ASTM E399-78), and the obtained K_Q value decreases with the increase of the test temperature. The K_Q value is not the real LEFM K_{1c} value because the criterion of $P_{max}/P_Q < 1.1$ has not been satisfied. However, the corresponding J_Q obtained from the K_Q analysis is comparable to the J_{1c} obtained from the E813-81 method at lower temperature (−45 or −60°C), an indication of LEFM behavior at lower temperature. The various schemes and size criterion based on LEFM and the *J*-method are explored for the validity of J_{1c} and K_{1c} values. © 1996 John Wiley & Sons, Inc.

INTRODUCTION

The rapid development of critical applications of engineering plastics makes it desirable to have practical and reproducible measurements of fracture toughness that can be used in engineering design. Most of the research work on the fracture of plastic materials has so far centered around the linear elastic fracture mechanics (LEFM) approach, employing the elastic analysis of the crack tip region. Conventional fracture criteria, such as the K_{1c} or G_{1c} values, derived from linear elastic fracture mechanics analysis have been successfully applied to those relatively brittle polymers such as polystyrene (PS) and poly(methyl methacrylate) (PMMA). However, linear elastic fracture mechanics is not suitable for most rubber-toughened polymeric materials because the problem of extensive plasticity at the crack tip has precluded the application of the criteria. Besides, a relatively larger specimen thickness required for LEFM to induce plane strain conditions is inconvenient experimentally. The path-independent contour integral (*J*-integral) approach was proposed by Rice as a two-dimension energy line integral that can be used as an analytical tool to characterize the crack tip stress and strain field under both elastic and plastic stress and strain.[1] Begley and Landes applied the *J*-integral principle and developed a measurement of fracture toughness, J_{1c}, which represents the energy required to initiate crack growth.[2,3] Since then, two key ASTM standards, E813-81 and E813-87, have been established for *J*-testing mainly for metallic materials.[4,5] These two ASTM E813 standards have been used to characterize toughened polymers and blends during last decade.[6–20] Seidler and Grellmann studied the fracture behavior and morphologies of PC/ABS blends using a special technique, a stop block method.[20] It

* To whom correspondence should be addressed.

Journal of Applied Polymer Science, Vol. 62, 863–874 (1996)
 CCC 0021-8995/96/060863-12

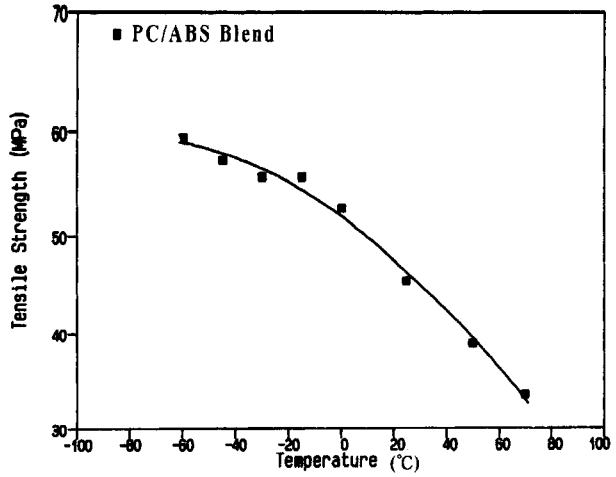

Figure 1 Plot of tensile yield strength vs. temperature.

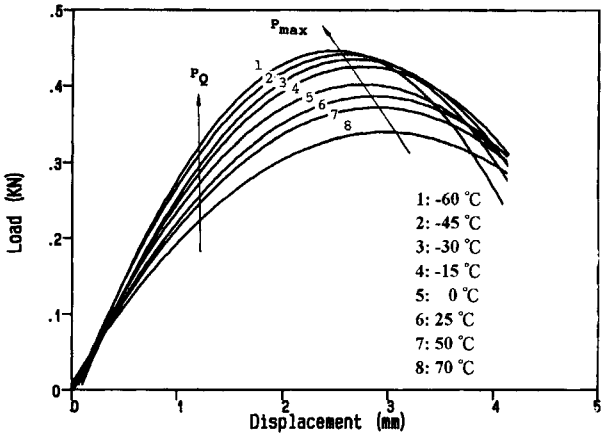

Figure 3 Plots of load–displacement curves at different temperatures.

was shown that the PC/ABS blends exhibit a very different fracture behavior depending on temperature and ABS content. Narisawa and Takemori studied several rubber-modified polymers and raised questions about the validity of the crack blunting line equation since the blunting phenomenon was not being observed.[21] Huang and Williams suspected that the crack face may close due to plasticity-induced crack closure, completely obscuring any blunting of the crack tip.[22,23] Huang later studied the *in situ* SEM crack growth on rubber-toughened nylon 6,6 and did observe the crack blunting but the growing process was not identical to that proposed for metals.[23] When a precrack specimen of a toughened polymer is under load, viscoelastic and inelastic micromechanisms such as craze, cavitation, debonding, and shear yielding may occur significantly around the crack tip region. These above-mentioned micromechanisms occur during the processes of crack tip blunting (precrack) and during crack propagation.[24-28] The crack tends to propagate within the plastic zone and results in a stable crack extension for the rubber-toughened polymer materials. In our recent studies to determine the fracture toughness of the elastomer-toughened polycarbonate, acrylonitrile–butadiene–styrene (ABS), and high-impact polystyrene (HIPS), an unconventional approach on the J-integral based on the above-mentioned hysteresis properties was employed.[24-28] The J_{1c} values obtained based on this hysteresis energy method are very close to those obtained from the ASTM E813-81 method but are significantly lower than those from the ASTM E813-87 method.

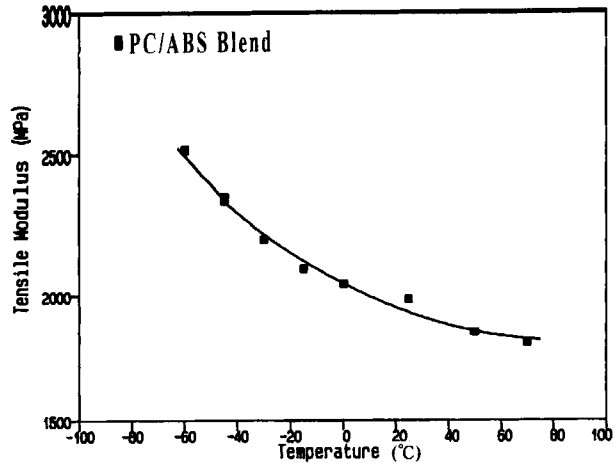

Figure 2 Plot of tensile modulus vs. temperature.

CHARACTERIZING PARAMETERS OF FRACTURE MECHANICS

The Linear Fracture Parameters K_{1c} and G_{1c}

The theory of LEFM deals with crack initiation occurring at nominal stresses that are well below the uniaxial yield stress of the material. A precrack specimen with little plastic deformation can be carried out by LEFM to measure the fracture toughness, K_{1c}, which characterizes the elastic field around the crack tip. For a single-edge notched bending (SENB) specimen by loading monotonically, its K_{1c} is given by the K_Q analysis[29]:

$$K_Q = (P_Q S/BW^{3/2})\, Y(a/W) \qquad (1)$$

where $Y(a/W)$ is a geometrical correction factor, P_Q is the 5% slope offset gross applied stress, and a, B, and W are the initial crack length, thickness, and

width of the specimen, respectively. For an SENB specimen with $S/W = 4$, the geometrical correction factor is given by

$$Y(a/W) = \frac{3 \times (a/W)^{1/2}\{1.99 - (a - W)(1 - a/W_2) \times [2.15 - 3.93(a/W) + 2.7(a/W)^2]\}}{2 \times [1 + 2(a/W)](1 - a/W)^{3/2}} \quad (2)$$

K_{1c} is related to the strain energy release rate of the fracture G_{1c} by the following equation:

$$K_{1c}^2 = E \times G_{1c}/(1 - \nu^2) \quad (3)$$

where E is the elastic modulus and ν is the Poisson's ratio.

The *J*-Integral

The fracture toughness based on the J-integral can be expressed as follows:

$$J = \int_r \left[Wdy - \bar{T} \times \frac{\partial \bar{U}}{\partial x} ds \right] \quad (4)$$

where the T is the surface traction; W, the strain energy density; U, the displacement vector; and x and y are the axis coordinates. Physically, the J-integral can be expressed in terms of energy as

$$J = -dU/Bda \quad (5)$$

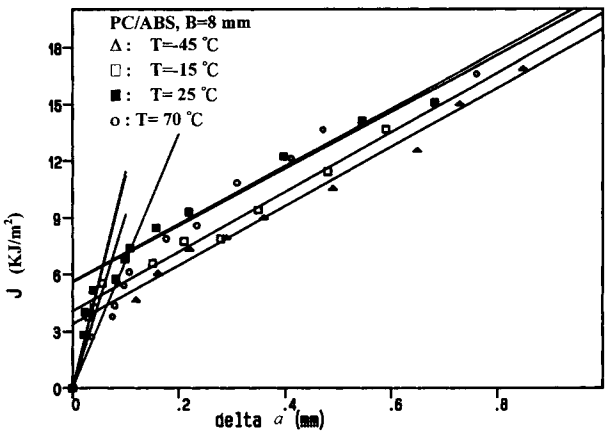

Figure 4 Plots of J vs. Δa according to ASTM E813-81 method at a few selected temperatures.

where B is the thickness of the loaded body, and a, the crack length. U is the total potential energy which can be obtained by measuring the area under the load-displacement curve. This equation can be further expressed by following equation[30,31]:

$$J = J_e + J_p \quad (6)$$

J_e and J_p are the elastic and plastic components of the total J value which can be represented by the following equations:

$$J_e = \eta_e \times U_e/B \times (W - a) \quad (7)$$

$$J_p = \eta_p \times U_p/B \times (W - a) \quad (8)$$

Table I Summarized *J* Data for a Typical PC/ABS Blend at $T = -15°C$

D (mm)	Input Energy (J)	J (kJ/m^2)	Hysteresis Ratio (%)	Hysteresis Energy (J)	a (mm)
1.1	0.138	3.750	2.28	0.0031	0.030
1.2	0.155	4.212	3.62	0.0056	0.041
1.3	0.202	5.489	5.46	0.0110	0.056
1.5	0.244	6.630	7.23	0.0176	0.151
1.6	0.286	7.772	9.72	0.0278	0.212
1.7	0.291	7.908	9.88	0.0288	0.283
1.8	0.345	9.375	13.79	0.0476	0.352
2.0	0.422	11.467	18.39	0.0776	0.485
2.2	0.503	13.668	22.06	0.1110	0.591
2.4	0.609	16.049	26.05	0.1580	0.687
2.6	0.666	17.598	30.29	0.2017	0.820
2.7	0.735	19.973	33.76	0.2481	0.991
2.8	0.784	21.304	36.62	0.2871	1.162
3.0	0.847	23.016	43.93	0.3721	1.224
3.2	0.950	25.815	47.51	0.4513	1.383

D: deformation displacement. J: $J = 2U/B \times b$. Δa: measured crack growth length.

Table II Critical J from the ASTM E813-81 and the LEFM Compliance Methods

	Temp							
	70°C	50°C	25°C	0°C	−15°C	−30°C	−45°C	−60°C
J_{1c} (kJ/m^2)	7.33	6.66	6.72	5.91	4.78	4.54	3.83	3.36
J_0 (kJ/m^2)	5.63	5.24	5.61	5.04	4.07	3.98	3.37	2.96
J_i (kJ/m^2)	3.45	5.49	4.61	5.65	4.10	2.17	3.87	3.58

J_{1c}: standard ASTM E813-81 method. J_0: modified version of ASTM E813-81 method by intercepting blunting line with Y-axis. J_i: LFEM compliance method.

U_e and U_p are the elastic and plastic components of the total energy. η_e and η_p are their corresponding elastic and plastic work factors. $(W - a)$ is the ligament length, and W, the specimen width. For a three-point bend single-edge notched specimen with $a/W > 0.15$, η_p is equal to 2. When the specimen has a span of $4W$ ($S = 4W$) and $0.4 < a/W < 0.6$, η_e is equal to 2. Therefore, eq. (5) can be reduced to

$$J = 2 \times U/B \times b \tag{9}$$

The crack growth resistance (R curve) is obtained by plotting the J values against the corresponding Δa values.

In the ASTM E813-81 standard, the critical J value for crack initiation, J_{1c}, is determined by intersecting the linear regression R curve and the crack blunting line. The blunting line can be expressed by the following equation:

$$J = 2 \times m \times \sigma_y \times \Delta a \tag{10}$$

where Δa is the crack growth length, and m, a constraint factor ($m = 1$ for plane stress and $m = 2$ for plane strain). Two lines parallel to the crack blunting line at an offset of $0.006b$ and $0.06b$ (mm) are drawn, respectively, as the minimum and maximum crack extension lines.[4]

In the ASTM E813-87 standard, instead of a bilinear fit lines, the J-Δa curve is then fitted by a power law with the following equations[5]:

$$J = C_1 \times (\Delta a)^{C2} \tag{11}$$

$$\ln J = \ln C_1 + C_2 \ln \Delta a \tag{12}$$

The critical J value, J_{1c}, is now at the intersection of the power law fitted line and the 0.2 mm blunting offset line of the following equation:

$$J = 2\sigma_y \times \Delta a - 0.4\sigma_y \tag{13}$$

J-Δa Curve from LEFM Compliance Method

Analysis of the J-Δa data using the LEFM theory by assuming negligible plasticity occurring in a specimen was previously proposed.[32] That means that all the nonlinearity in the load–displacement curve is due solely to the crack extension. In this

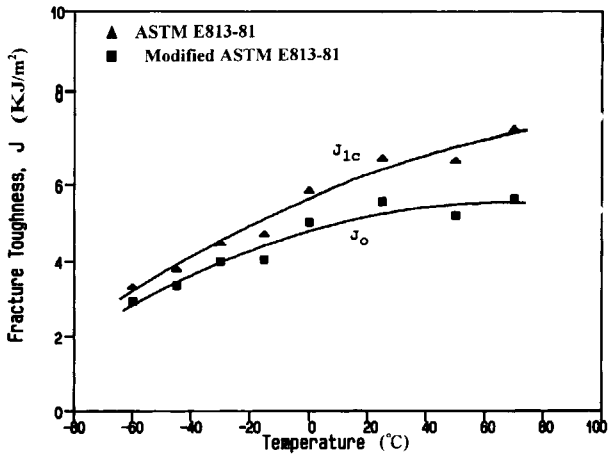

Figure 5 Plots of critical fracture toughness J vs. temperature from ASTM E813-81 and its modified methods.

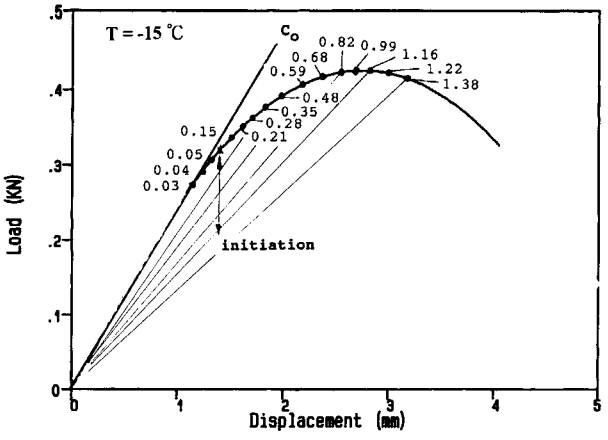

Figure 6 Plot of load vs. displacement and corresponding Δa at $T = -15$°C.

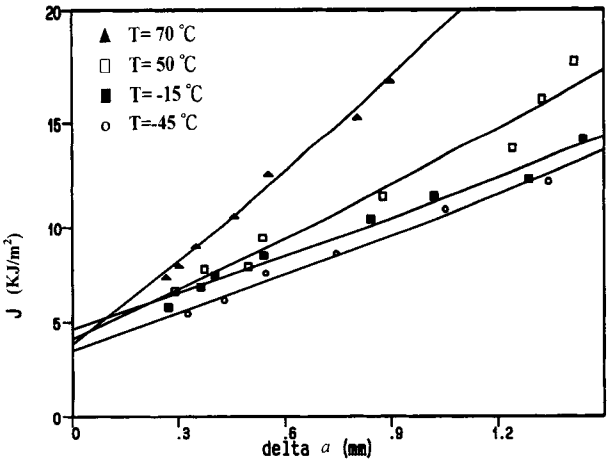

Figure 7 Plots of J vs. Δa according to LEFM compliance method at different temperatures.

situation, the Δa can be determined theoretically from a compliance measurement at any point along the load–displacement curve. The energy calibration factor, Φ, in an elastic body is given by[31]

$$\Phi = (C/W)/(dC/da) \tag{14}$$

where C is the compliance of the body. For the SENB specimen with $S/W = 4$, the $(1 - a/W)/\Phi$ is equal to 2. The equation[14] becomes

$$da/(W - a) = 0.5\, dC/C \tag{15}$$

Integration of eq. (15) gives

$$\Delta a = (W - a_0)[1 - (C_0/C)^{1/2}] \tag{16}$$

where C_0 is the compliance at $a = a_0$.

J-Integral According to Hysteresis Energy Method

Hysteresis defined in this method is not exactly same as the conventional definition; it is the energy difference between the input and the recovery in the cyclic loading and unloading steps which may include crack blunting and crack extension stages. The close relation between the precrack hysteresis and the corresponding ductile–brittle transition behavior of polycarbonate and polyacetal was previously reported.[33-36] When a precrack specimen is under loading before the onset of crack extension (during blunting), a significant portion of the input energy is consumed and converted into a relatively larger crack tip plastic zone for the toughened polymers. These viscoelastic and inelastic energies may include many possible energy dissipated micromechanisms such as craze, cavitation, debonding, and shear yielding which can be related to the measured hysteresis energy. The hysteresis energy will increase gradually with the increase of load from the load vs. displacement curve. After crack extension, the strain energy release due to crack growth will add into the observed total hysteresis energy. The rate of hysteresis energy increase due to this strain energy release is significantly higher than those above-mentioned precrack micromechanisms. Therefore, in a plot of hysteresis energy vs. deformation displacement of a notched specimen, a clear transition from crack blunting to crack extension can be identified. Such a phenomenon, a drastic increase of the hysteresis energy immediately after the onset of the crack extension, can be used to determine the critical fracture toughness (J_{1c}) as the onset of crack extension. The data observed to support the this viewpoint were presented in our previous articles.[24-28]

The J_{1c} Validity Requirements

For fracture toughness to be characterized as J_{1c}, a specimen must meet certain size requirements to achieve a plane strain stress state along the crack front. To achieve this stress state, all specimen dimensions must exceed some multiple of J_{1c}/σ_y. According to ASTM E813,[4,5] a valid J_{1c} value may be obtained whenever

$$B, \quad (W - a), \quad W > 25(J_{1c}/\sigma_y) \tag{17}$$

and

$$dJ/da < \sigma_y \tag{18}$$

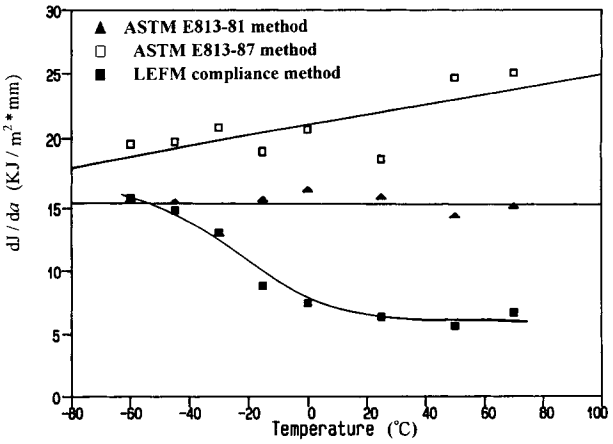

Figure 8 Plots of dJ/da vs. temperature from ASTM E813-81, E813-87, and LEFM compliance methods.

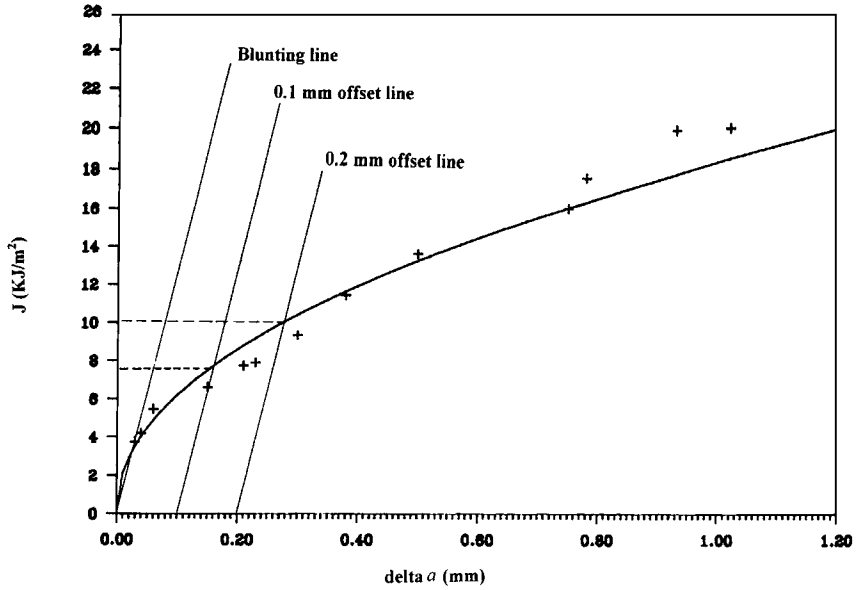

Figure 9 J-integral by ASTM E813-87 method at $T = -15°C$.

where the slope of power law regression line of E813-87, dJ/da, is evaluated at $\Delta a = 0.2$ mm. Paris and co-workers[37] developed the tearing modulus concept to describe the stability of a ductile crack in term of elastic–plastic fracture mechanics. This fracture instability occurs if the elastic shortening of the system exceeds the corresponding plastic lengthening for crack extension. A nondimensional parameter, tearing modulus (T_m), has been defined as the following equation[37]:

$$T_m = (dJ/da) \times (E/\sigma_y^2) \tag{19}$$

Furthermore, for the J-Δa data to be regarded as a material property independent of specimen size, the criterion $\omega > 10$ must be met, where ω is defined as

$$\omega = (W - a)/J_{1c} \times dJ/da \tag{20}$$

Finally, for the plane strain linear elastic behavior, J_{1c} becomes identical to the critical strain energy release rate, G_{1c}, which is, in turn, related to the stress intensity factor, K_{1c}, used in linear elastic fracture mechanics:

$$J_{1c} = G_{1c} = (1 - \nu^2)K_{1c}^2/E \tag{21}$$

EXPERIMENTAL

The PC/ABS blend (Shinblend A783) was obtained from Shing-Kong Synthetic Fiberic Corp. of Taiwan. The tensile yield strength and Young's modulus were measured by using the standard injection-molded specimens ($\frac{1}{8}$ in.) with an extensometer. The Poisson's ratio of the PC/ABS is assumed to be 0.35. Test specimens are the three-point bending bars with dimensions of $B = 8$ mm, $W = 20$ mm, and L

Table III Critical J from the ASTM E813-87 Methods

	Temp							
	70°C	50°C	24°C	0°C	−15°C	−30°C	−45°C	−60°C
C_1	1689	573	279	498	408	2043	1088	1099
C_2	0.629	0.496	0.399	0.476	0.456	0.683	0.599	0.602
J_{1c} (kJ/m²)	12.15	11.88	11.32	11.2	10.01	7.30	7.92	7.73
J_0 (kJ/m²)	8.83	8.35	9.42	8.79	7.73	7.30	5.27	5.33

J_{1c}: standard ASTM E813-87 method. J_0: modified version of E813-87 by using 0.1 mm offset line.

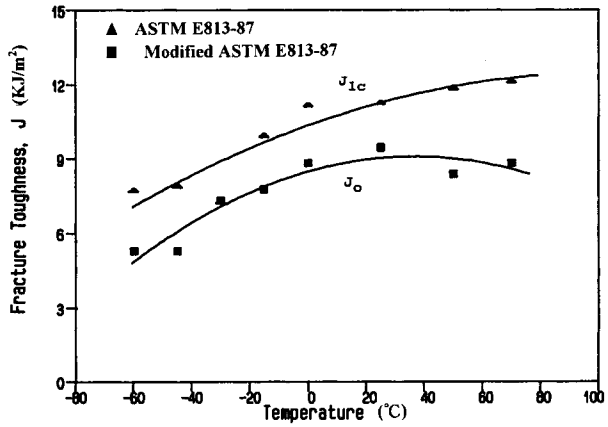

Figure 10 Plots of the critical fracture toughness vs. temperature from ASTM E813-87 and its modified methods.

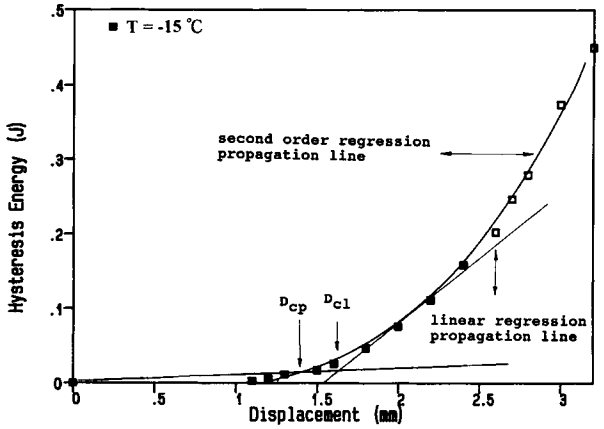

Figure 11 Plot of hysteresis energy vs. displacement at $T = -15°C$.

= 90 mm. Specimens with a single-edge notch of the initial crack length, a, of 10 mm ($a/W = 0.5$) were prepared by injection molding using an Arburg injection-molding machine. The initial precrack was followed by sharpening with a fresh razor blade. All the notched specimens were annealed at a temperature slightly higher than the T_g of the material for 2–3 h to release the possible residual stress prior to the standard bending tests. The J-method was carried out according to the ASTM E813 method at a crosshead speed of 2.0 mm/min by using an Universal tensile test machine (Instron Model 4201). The test temperatures were controlled at 70, 50, 25, 0, −15, −30, −45, and −60°C, respectively, with an accuracy of +1°C by an Instron temperature controller. The specimens were loaded to various displacements corresponding to different crack growth lengths and then unloaded at same test rate. After unloading, the specimens were frozen in liquid nitrogen and broken open by a TMI impacter. The crack growth length, Δa, was measured of the broken specimen by using a traveling optical microscope. The fracture and hysteresis energies of each test specimen were obtained by measuring the area under the load-displacement curve and energy loss from the loading–unloading loop, respectively.

RESULTS AND DISCUSSION

J_{1c} Determination by ASTM Standards and the Modified Versions

Figure 1 shows the plot of tensile yield strength vs. temperature of the PC/ABS blend, where the yield strength decreases with the increase of temperature as would be expected. Figure 2 shows the plot of tensile modulus vs. temperature, where the modulus also decreases with increase of temperature. The load–displacement curves of the notched specimens of the PC/ABS blend at different temperatures are shown in Figure 3. The specimen at lower temperature has a considerably greater maximum load (P_{max}) than that at higher temperature due mainly to the higher modulus and higher yield stress. The J value for each specimen is calculated from eq. (9), and the corresponding crack growth, Δa, is measured from the fracture surface of the broken specimen. Detailed data of the specimens measured at $T = -15°C$ are summarized in Table I. Figure 4 shows the plots of the acceptable J vs. Δa by linear regression R curves according to the ASTM E813-81 method from a few selected temperatures. The linear regression R curves intercept with the corresponding blunting lines [eq. (10)] to locate the J_{1c} values. Another critical J value (J_0) is determined at the

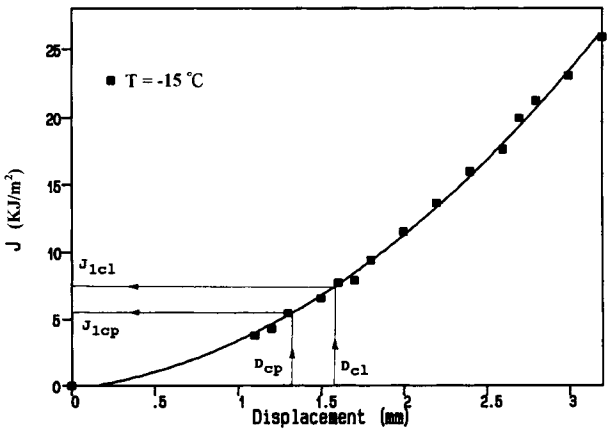

Figure 12 Plot of J vs. displacement at $T = -15°C$.

Table IV Critical Displacement and Critical J from the Hysteresis Energy Method

	Temp							
	70°C	50°C	25°C	0°C	−15°C	−30°C	−45°C	−60°C
D_{cl} (mm)	1.76	1.80	1.67	1.59	1.52	1.41	1.41	1.21
J_{1cl} (kJ/m^2)	7.61	8.38	7.55	7.54	7.07	6.10	6.58	4.38
D_{cp} (mm)	1.67	1.59	1.51	1.42	1.33	1.26	1.18	1.10
J_{1cp} (kJ/m^2)	6.98	6.96	6.33	6.16	5.55	5.33	5.17	5.13
D_ca (mm)	1.62	1.62	1.51	1.38	1.30	1.16	—	—

D_c: critical initial displacement. l: from the plot of hysteresis energy vs. displacement by using the linear propagation line. p: from the plot of hysteresis energy vs. displacement by using the power law propagation line. a: from the plot of the measured crack growth length vs. displacement.

interception of the linear regression resistance curve with the Y-axis as recommended by Narisawa and Takemori.[21] The J_0 obtained is slightly lower than that from the E813-81 method as would be expected. All these data from ASTM E813-81 (J_{1c}) and the modified method (J_0) are summarized in Table II. Figure 5 shows the plots of J_{1c} and the J_0 value vs. temperature; both J_{1c} and J_0 increase with increase of temperature. The actual fracture process itself is very complex: The point of first crack advance (at which J_{1c} or J_0 is defined) is difficult to ascertain even by direct observation of the fracture surface subsequent to fracture.

The plot of the load vs. displacement curve at T = −15°C is shown in Figure 6, where the experimentally obtained crack growth lengths (Δa) are labeled on the curve. The onset of crack initiation by ASTM E813-81 in this load–displacement curve is located near the beginning of the nonlinearity of the curve. For the LEFM compliance method, the Δa is calculated by using eq. (16) along the load–displacement curve shown in Figure 8 at T = −15°C.

Figure 7 shows the plots of the Δa calculated from eq. (16) vs. corresponding J values at different temperatures. The calculated Δa value from eq. (16) is significantly higher than the actually measured Δa value from the fractured surface. The cause of the observed difference is due to the neglect of the plasticity under testing. Figure 8 shows the plots of dJ/da from the ASTM E813-81, E813-87, and the LEFM compliance methods vs. temperature. The obtained dJ/da values from the LEFM compliance method are substantially lower than those obtained from the ASTM E813-81 except at lower temperatures (T = −45°C and T = −60°C). The fracture behavior of the rubber-toughened polymer is gradually approaching to meet the LEFM conditions at low temperatures, near or below the T_g of the rubber. Moskala[38] studied the core–shell rubber-modified polycarbonate by comparing Δa from ASTM E813 and LEFM compliance methods at various temperatures and came to similar conclusions. This result is not unexpected since the LEFM compliance

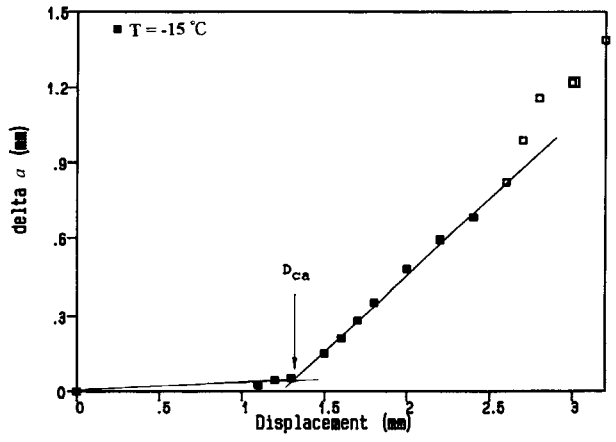

Figure 13 Plot of the truly crack growth length (Δa) vs. displacement at T = −15°C.

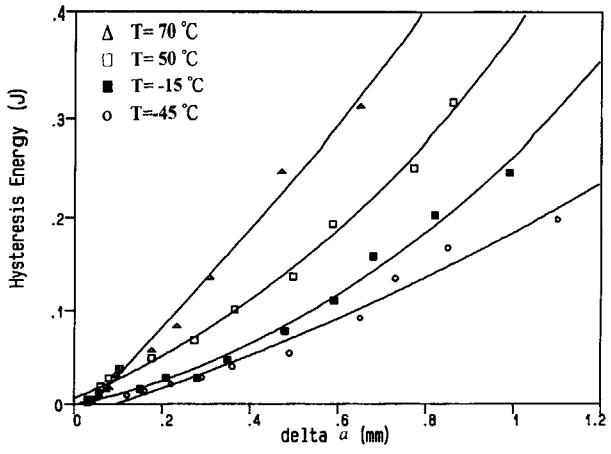

Figure 14 Plots of the hysteresis energy vs. the crack growth length from a few selected temperatures.

Table V The Size Criterion Requirements for Valid J_{1c} Value

	Temp							
	70°C	50°C	25°C	0°C	−15°C	−30°C	−45°C	−60°C
ASTM E813-81 method								
$dJ/d\alpha$	15.22	14.51	15.97	16.33	15.73	13.09	15.56	15.79
$25(J_{1c}/\sigma_y)$	5.47	4.28	3.68	2.80	2.18	2.03	1.67	1.41
T_m	24.57	17.73	15.19	12.04	10.94	9.37	11.23	11.21
ω	20.76	21.78	23.76	27.63	32.90	28.70	40.62	46.90
$\omega > 10$	Yes	Yes	Yes	Yes	Yes	Yes	Yes	Yes
Plane strain	Yes	Yes	Yes	Yes	Yes	Yes	Yes	Yes
ASTM E813-87 method								
$dJ/d\alpha$	25.02	24.64	18.61	20.6	19.03	20.76	19.83	19.62
$25(J_{1c}/\sigma_y)$	9.06	7.63	6.21	5.31	4.05	3.27	3.46	3.24
T_m	40.39	30.12	17.70	15.19	13.23	14.86	14.31	13.93
ω	20.59	20.74	16.43	18.39	19.03	28.43	25.03	25.30
$\omega > 10$	Yes	Yes	Yes	Yes	Yes	Yes	Yes	Yes
Plane strain	Yes	Yes	Yes	Yes	Yes	Yes	Yes	Yes

$T_m = E/\sigma_y^2\, dJ/d\alpha$. $\omega = (W - \alpha)/J_{1c} \times dJ/d\alpha$.

method attributes all the nonlinearity to the elastic crack extension and neglects the occurrence of the inelasticity or the plasticity.

In ASTM E813-87 method, the J_{1c} is located at the intercept between the power law fit line and the 0.2 mm offset line as shown in Figure 9 at $T = -15$°C. The values of C_1 and C_2 of the power law regression line, $J = C_1 \times \Delta a^{C_2}$, within 0.15 and 1.5 mm exclusion lines, and the corresponding J_{1c} values at different temperatures ranging from −60 to 70°C are summarized in Table III. The J_{1c} values obtained from the E813-87 method are about 80–110% higher than those from the corresponding E813-81 method (Table II). The critical J_{1c} definition has been and still is a confusing and controversial issue, whether it is treated as crack initiation (E813-81) or is simply an engineering definition for design purpose (E813-87). Only very limited comparative J_{1c} data between these two ASTM standards (E813-81 and E813-87) on polymeric materials have been previously reported. Huang[23] recently reported that the J_{1c} from the E813-87 method for the rubber-toughened nylon 6,6 is significantly higher than that from the E813-81 method (38 vs. 15 kJ/m^2). We also found that the J_{1c} values obtained from the E813-87 method for the elastomer-modified polycarbonate[24] and high-impact polystyrene[26] are about 20–40% higher than those from the E813-81 method. However, if the 0.2 mm offset line specified in E813-87 is now reset at 0.1 mm and the rest of the procedures remain

Table VI The K_Q Analysis Based on ASTM E399-78 Method

Temp (°C)	P_Q (kN)	P_{max} (kN)	P_{max}/P_Q	K_Q (Mpa × $a^{1/2}$)	J_Q (kJ/m^2)
70	0.2282	0.3418	1.50	2.15	2.24
50	0.2512	0.3747	1.49	2.36	2.64
25	0.2608	0.3902	1.49	2.45	2.66
0	0.2786	0.4405	1.45	2.61	2.92
−15	0.2939	0.4265	1.45	2.76	3.11
−30	0.3020	0.4261	1.41	2.84	3.18
−45	0.3187	0.4452	1.39	2.99	3.32
−60	0.3280	0.4515	1.37	3.08	3.31

P_Q: the load at 5% slope offset line. P_{max}: the maximum load. K_Q : $K_Q = (P_Q S/BW^{3/2})\ Y(\alpha/W)$. J_Q : $J_Q = (1 - \nu^2)\ K_Q^2/E$, the K_Q corresponding J value.

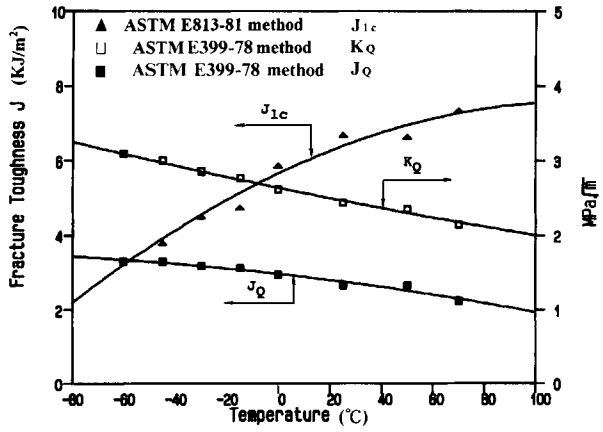

Figure 15 Plots of the critical fracture toughness according to the E813-81 and E399-78 methods vs. temperature.

unchanged as shown in Figure 9, the critical J_0 values obtained from the E813-87 modified method are now only slightly higher than those obtained from the E813-81 method (Table II). Similar results were also obtained from elastomer-modified polycarbonate,[24] high-impact polystyrene,[26] and acrylonitrile–butadiene–styrene.[25] After all, the 0.2 mm offset line suggested in the ASTM E813-87 standard is only an arbitrarily selected value to define the critical fracture toughness (J_{1c}). Figure 10 shows the plots of the J_{1c} from the E813-87 method and the J_0 from the E813-87 modified method vs. temperature; both J_{1c} and J_0 increase with increase of the temperature.

J_{1c} Determination from the Hysteresis Method

The hysteresis ratio and the corresponding hysteresis energy of each specimen at different displacements are summarized in Table I for $T = -15°C$. Figure 11 shows the plot of the hysteresis energy vs. crosshead displacement at $T = -15°C$. The critical initiation displacement is located at the intersection between the blunting line and the linear crack propagation line, namely, D_{cl} (the validity crosshead displacement data window is used with its corresponding crack growth length, Δa, ranging from 0.10 to 0.80 mm) or the second-order power law crack propagation line, namely, D_{cp} (the validity crosshead displacement data window is used with its corresponding crack growth length, Δa, ranging from 0.10 to 1.50 mm). As soon as the D_{cl} and D_{cp} are located, their corresponding J_{1c} values (namely, J_{1cl} and J_{1cp}) are then determined from the plot of the J vs. crosshead displacement curve as shown in Figure 12, respectively. Because the measurement of crack growth length (Δa) is no longer necessary by this hysteresis energy method, it is relatively easier than the conventional ASTM E813 methods. The J_{1c} values, (J_{1cl} and J_{1cp}) obtained from the hysteresis energy method are very close to those from the E813-81 method (Table II), but lower (60–80%) than those from the E813-87 method (Table III). The critical J_{1cp} values are relatively closer to the J_{1c} values obtained from the E813-81 method than are the J_{1cl} values. Therefore, the critical initiation displacement (D_{cp}) is probably better related to the true crack initiation than is D_{cl}. Our previous articles used D_{cl} instead of D_{cp} in determining J_{1c}.[24–27] The obtained D_{cl}, D_{cp}, J_{1cl}, and J_{1cp} values are summarized in Table IV. The critical J value determined by this unconventional hysteresis energy method has its physical meaning as the onset of crack extension rather than that based on the theoretically predicted blunting line as in the ASTM E813-81 method or that based on an arbitrarily chosen engineering definition as in the ASTM E813-87 method. A plot of the experimentally measured crack growth length (Δa) vs. crosshead displacement is shown in Figure 13 at $T = -15°C$. The critical initiation displacement is now located at the intersection of these two linear regression lines. The critical initiation displacements, D_c's, obtained from these two methods, the hysteresis energy and the crack growth length vs. displacement, are fairly close (Table IV). This coincident result implies that the critical initiation displacement determined from the hysteresis method is indeed the true onset of crack extension. Figure 14 shows the plots of the hysteresis energy vs. corresponding crack growth length, Δa, from a few selected temperatures. The slope from the curve increases with the increase of temperature, which indicates that additional energy is required to extend the same crack growth length at higher temperature than at lower temperature in the forms of more craze and more localized shear yielding during crack growth. Therefore, more energy in terms of hysteresis energy is required for crack growth at higher temperature.

The Size Criterion of Specimens

The dJ/da values obtained according to the linear regression R curves of ASTM E813-81 and the power law regression curve of ASTM E813-87 at $\Delta a = 0.2$ mm are summarized in Figure 8 and Table V. The dJ/da value obtained from the E813-87 method increases gradually with increase of temperature while the dJ/da value from the E813-81 method is fairly temperature-independent. Overall, the dJ/da values from the E813-87 method are about 30–60% higher

than those from the E813-81 method. Tearing modulus, T_m, is used to describe the stability of the crack growth. Table V shows that the tearing modulus T_m value increases with the increase of temperature which indicates greater crack propagation resistance at higher temperature. For the $J-\Delta a$ data to be regarded as an intrinsic material property independent of specimen size, the critical parameter of $\omega > 10$ must be met. In this study, all specimen dimensions employed meet the ASTM size criterion, $\omega > 10$, and the obtained ω parameter increases with decrease of temperature as shown in Table V. Other size requirements such as those of eq. (17) have also been satisfied. The size criteria produce a plastic plane-strain stress condition at the crack front and allow for the use of significantly smaller specimen dimensions than those required for LEFM testing. Table V summarizes the different size criterion values and essentially all these criteria meet requirements of the validity J_{1c} test in this study.

The K_Q Analysis

A typical load–displacement curve for a precrack bending specimen at different temperatures is shown in Figure 3. The load P_Q is obtained from the 5% secant offset of the load–displacement curve (ASTM E399-78) which is used to calculate K_Q. Now, ASTM D5045 for plastics has replaced ASTM E399 for metallic materials, but ASTM E399 was the one discussed in this article.[40] If the amount of the plastic development is small at the running crack tip and the rate of the crack growth above P_Q is rapid, the corresponding K_Q is considered as a validity K_{1c}. For the criterion of a validity K_Q as a K_{1c}, the following relationships must be met:

$$B, \quad a, \quad (W-a) > 2.5(K_Q/\sigma_y)^2 \qquad (22)$$

$$P_{max}/P_Q < 1.10 \qquad (23)$$

where P_{max} is the maximum load on the load–displacement curve and σ_y is the yield strength. Table VI summarizes the K_Q and the corresponding J_Q values, which are determined by using eq. (21). Since all the P_{max}/P_Q values obtained do not meet the criterion of $P_{max}/P_Q < 1.1$ at temperatures ranging from −60 to 70°C, the corresponding K_Q values obtained cannot be considered as true K_{1c} values of LEFM. Figure 15 shows the plots of the K_Q, J_Q (from the ASTM E399-78) and J_{1c} (from the E813-81) vs. temperature. Both K_Q and J_Q decrease with the increase of the temperature, while the corresponding J_{1c} increases with increase of temperature. At low temperature (−60°C), J_{1c} and J_Q are nearly identical, an indication of LEFM behavior.

CONCLUSION

The J_{1c} values obtained from the hysteresis energy method using the critical initiation displacement D_{cp}'s are comparable to those obtained from the E813-81 method but are about 70–90% lower than those obtained from the E813-87 method. All these critical J values obtained from ASTM E813-81, E813-87, and hysteresis energy methods increase with increase of temperature. From the ASTM E399-78 method, the K_Q values are not the real LEFM K_{1c} values because the $P_{max}/P_Q < 1.1$ criterion is not met. However, the corresponding J_Q values are comparable to those obtained from the E813-81 method at lower temperatures, an indication of LEFM behavior. The specimen geometry of this study essentially meets all the size criterion, and, therefore, the J_c's obtained are considered to be valid. The hysteresis energy method inherently adjusts for the occurrence of the crack blunting and thus avoids the controversy of the blunting line issue. Besides, it is simple without the requirement of the tedious crack growth length measurements.

The authors are grateful to the National Science Council of Republic of China for the financial support and Shingkong Synthetic Fiberic Corp. of Taiwan for the PC/ABS blend samples.

REFERENCES

1. J. R. Rice, *J. Appl. Mech.*, **35,** 379 (1968).
2. J. A. Begley and J. D. Landes, ASTM STP 514, 1 (1972).
3. J. D. Landes and J. A. Begley, ASTM STP 560, 170 (1974).
4. ASTM Standard E813-81, *Annual Book of ASTM Standards,* 1981, Part 10, p. 810.
5. ASTM Standard E813-87, *Annual Book of ASTM Standards,* 1987, Part 10, p. 968.
6. M. K. V. Chan and J. G. Williams, *Int. J. Fract.*, **19,** 145 (1983).
7. M. K. V. Chan and J. G. Williams, *Polym. Eng. Sci.*, **21,** 1019 (1981).
8. S. Hashemi and J. G. Williams, *Polymer,* **27,** 85 (1986).
9. D. D. Huang and J. G. Williams, *J. Mater. Sci.*, **22,** 2503 (1987).
10. P. K. So and L. J. Broutman, *Polym. Eng. Sci.*, **26,** 1173 (1986).

11. E. J. Moskala and M. R. Tant, *Polym. Mater. Sci. Eng.*, **63,** 63 (1990).
12. C. M. Rimnac, T. M. Wright, and R. W. Klein, *Polym. Eng. Sci.*, **28,** 1586 (1988).
13. I. Narisawa, *Polym. Eng. Sci.*, **27,** 41 (1987).
14. D. S. Parker, H. J. Sue, J. Huang, and A. F. Yee, *Polymer*, **31,** 2267 (1990).
15. Y. W. Mai and B. Cotterell, *J. Mater. Sci.*, **15,** 2296 (1980).
16. Y. W. Mai and B. Cotterell, *Eng. Fract. Mech.*, **21,** 123 (1985).
17. J. Wu, Y. W. Mai, and B. Cotterell, *J. Mater. Sci.*, **28,** 3373 (1993).
18. N. Haddaoui, A. Chudnovsky, and A. Moet, *Polymer*, **27,** 1337 (1986).
19. I. C. Tung, *Polym. Bull.*, **25,** 253 (1991).
20. S. Seidler and W. Grellman, *J. Mater. Sci.*, **28,** 4078 (1993).
21. I. Narisawa and M. T. Takemori, *Polym. Eng. Sci.*, **29,** 671 (1989).
22. D. D. Huang and J. G. Williams, *Polym. Eng. Sci.*, **30,** 1341 (1990).
23. D. D. Huang, *Polym. Mater. Sci. Eng.*, **63,** 578 (1990).
24. C. B. Lee and F. C. Chang, *Polym. Eng. Sci.*, **32,** 792 (1992).
25. M. L. Lu, C. B. Lee, and F. C. Chang, *Polym. Eng. Sci.*, **35,** 1433 (1995).
26. C. B. Lee, M. L. Lu, and F. C. Chang, *J. Appl. Polym. Sci.*, **47,** 1867 (1993).
27. M. L. Lu and F. C. Chang, *Polymer*, **36,** 2541 (1992).
28. M. L. Lu and F. C. Chang, *J. Appl. Polym. Sci.*, **56,** 1065 (1995).
29. ASTM Standard E399-78, *Annual Book of ASTM Standards*, 1978, Part 10, p. 540.
30. J. D. Sumpter and C. E. Turner, *Int. J. Fract.*, **9,** 320 (1973).
31. J. G. Williams, *Fracture Mechanics of Polymers*, Ellis Horwood, Chichester, 1987.
32. J. D. Landes and J. A. Begley, ASTM STP 560, 170 (1974).
33. F. C. Chang and H. C. Hsu, *J. Appl. Polym. Sci.*, **43,** 1025 (1991).
34. F. C. Chang and M. Y. Yang, *Polym. Eng. Sci.*, **30,** 543 (1990).
35. F. C. Chang and H. C. Hsu, *J. Appl. Polym. Sci.*, **47,** 2195 (1993).
36. F. C. Chang and H. C. Hsu, *J. Appl. Polym. Sci.*, **52,** 1891 (1994).
37. P. C. Paris, H. Tada, A. Zahoor, and H. Ernst, ASTM STP 668, 5 (1979).
38. E. J. Moskala, *J. Mater. Sci.*, **27,** 4883 (1992).
39. ASTM Standard D5045-93, *Annual Book of ASTM Standards*, 310 (1994).

Received December 12, 1995
Accepted April 26, 1996